Available online at www.sciencedirect.com
ScienceDirect
International Journal of Heat and Mass Transfer 50 (2007) 4342–4351
International Journal of HEAT and MASS TRANSFER
www.elsevier.com/locate/ijhmt

Heat transfer and friction factor correlation for artificially roughened duct with metal grit ribs

S.V. Karmare [a,c,*], A.N. Tikekar [b,c]

[a] Department of Mechanical Engineering, Government College Engineering, Karad 415 124, Maharashtra, India
[b] Department of Mechanical Engineering, Walchand College of Engineering, Sangli, India
[c] Shivaji University, Kolhapur, Maharashtra, India

Received 19 August 2005; received in revised form 5 January 2007
Available online 13 June 2007

Abstract

This paper presents the results of an experimental investigation of heat transfer to the airflow in the rectangular duct of an aspect ratio 10:1. The top wall surface is made rough with metal ribs of circular cross section in staggered manner to form defined grid. The roughened wall is uniformly heated and the other walls are insulated. This geometry of duct closely corresponds to that used in solar air heaters. The effect of grit geometry [i.e., relative roughness height of grid (e/D_h), relative roughness pitch of grit (p/e), relative length of grit (l/s)] on the heat transfer coefficient and friction factor is investigated. The range of variation of system parameters and operating parameters is investigated within the limits, as e/D_h: 0.035 to 0.044, p/e: 12.5–36 and l/s: 1.72–1, against variation of Reynolds number: 4000–17,000. It is observed that the plate of roughness parameters $l/s = 1.72$, $e/D_h = 0.044$, $p/e = 17.5$ shows optimum performance. Correlations for Nusselt number and friction factor in terms of above parameters are developed which reasonably correlate the experimental data.

Keywords: Augmentation; Heat transfer; Roughness; Metal grid ribs; Turbulent

1. Introduction

The use of artificial roughness or turbulence promoters on a surface is an effective technique to enhance the rate of heat transfer to the fluid flowing in a duct [1]. However, it would result in an increase in frictional losses leading to more power required by fan or blower. In order to keep the friction losses at a minimum level, the turbulence must be created only in the region very close to the duct surface i.e., in laminar sub layer. The surface roughness can be produced by several methods, such as sand blasting, machining, casting, forming, welding or fixing ribs of small diameter wires to form a grid.

A number of investigations have been carried out on the heat transfer characteristics of channels or pipes with roughness elements on the surface. Nikuradse [2], Nunner [3] and Dipprey and Sabersky [4] have developed a friction similarity law and a heat momentum transfer analogy, for a flow in pipe with internal roughness. Han [5] carried out an experimental study for a fully developed turbulent airflow in square duct with two opposite walls roughened by ribs. Webb and Eckert [6] developed the heat transfer and friction factor correlations for turbulent air flow in tubes internally roughened by rib. Han and Zhang [7] investigated the effect of broken rib orientation on local heat transfer distribution and pressure drop in a square channel with two opposite walls roughened by ribs. Liou and Hwang [8] have investigated experimentally, the turbulent heat transfer and friction factor in a channel with ridges of various shapes mounted on two opposite walls.

* Corresponding author. Address: Department of Mechanical Engineering, Government College Engineering, Karad 415 124, Maharashtra, India. Tel.: +91 2164 272901; fax: +91 2164 271713.
E-mail address: karmaresv@rediffmail.com (S.V. Karmare).

0017-9310/$ - see front matter © 2007 Elsevier Ltd. All rights reserved.
doi:10.1016/j.ijheatmasstransfer.2007.01.065

Nomenclature

A_c	smooth plate heat transfer area, WL_f (m^2)
A_o	orifice area, πr^2 (m^2)
C_d	coefficient of discharge
C_p	specific heat of air (J/kg k)
D_h	hydraulic diameter of duct (m)
e	metal grid roughness height (mm)
e/D_h	relative roughness height
f	fanning friction factor
H	heat transfer coefficient (W/m^2 k)
H	air flow duct depth (mm)
K	thermal conductivity of air
L_f	length of test section (m)
l	projected length of metal grit perpendicular to direction of flow
s	projected length of metal grit parallel to direction of flow
l/s	relative length of metal grid
m	mass flow rate (kg/s)
Nu	Nusselt number
p	metal grid rib pitch (mm)
p/e	relative roughness pitch
Pr	Prandtl number
ΔP_o	pressure drop in orifice (Pa)
ΔP_d	pressure drop in duct (Pa)
Q	heat transfer rate (W)
Re	Reynolds number
St	Stanton number
T_a	ambient temperature (°C)
T_i	air inlet temperature (°C)
T_{fm}	bulk mean temperature (°C)
T_o	air outlet temperature (°C)
T_{pm}	mean plate temperature (°C)
T_1–T_5	plat temperatures (°C)
v	velocity of air (m/s) (m)
W	width of duct (m)
W/H	aspect ratio of duct (m)
Greek symbols	
ρ	density of air (kg/m^3)
θ	rib angle of attack (deg)

Prasad and Mullick [9] adopted artificial roughness in a solar air heater. The roughness was promoted by fixing small wires to increase the heat transfer surface. Prasad and Saini [10] investigated fully developed turbulent flow in a solar air heater duct with a small diameter profusion wire on the absorber plate. However, it is observed that the fixing of small wires on the absorber plate is a cumbersome task and may not be economically feasible [11]. A suitable geometry of roughness elements therefore needs to be selected, which is easily available and easy to fix on the absorber plate.

The literature survey reveals that no serious efforts have been made to investigate the possibility of reduction in frictional loss while increase in heat transfer. This paper presents experimental investigation of effect of increased roughness on heat transfer and frictional loss in a rectangular duct. One broad wall surface is roughened with ribs in defined grid geometry, which is exposed to uniform heat flux. The correlations for Nusselt number and friction factor in terms of roughness parameters are developed. The effect of system parameters [relative roughness height of grid (e/D_h), relative roughness pitch of grid (p/e), relative length of grid (l/s)] and operating parameter [Re] on friction factor and heat transfer is evaluated.

2. Experimental program

2.1. Experimental setup and procedure

The schematic layout of experimental setup is shown in Fig. 1. While preparing this setup norms recommended by ASHRAE Standards [12] are followed. The setup consisting of collector with necessary duct of aspect ratio 10 (250 mm × 25 mm) is provided with centrifugal blower to draw the air. Necessary measuring equipment and sensors are provided at appropriate locations (Thermocouple locations on the plate are shown in Fig. 2). To maintain length to hydraulic diameter ratio of more than 30 the proper test section length for collector is selected as 1.5 m [13]. Collector plates of aluminium with 1 mm thickness are selected on which artificial roughness is generated by fixing small diameter aluminum wires in pre-defined geometry. As an example, the geometry of plate no. 04 is shown in Fig. 3. Table 1 gives details of roughness parameters used for different collector plates.

For indoor testing the collector plate is provided with a nichrome wire heater of proper configuration to generate uniform heat flux on 1.5 m × 0.25 m. The whole test section is insulated after mounting the thermocouples at appropriate locations.

The test was conducted by keeping heat input constant and varying airflow such that the Reynolds number is maintained in the range of 4000–17,000 and required readings were recorded. All the readings are noted under steady state conditions. The steady state for each run was found to reach after about 1.5–2 h. This procedure was repeated for different plates.

2.2. Data reduction

Steady state value of the plate and air temperatures in the duct, at various locations for a given heat flux and mass

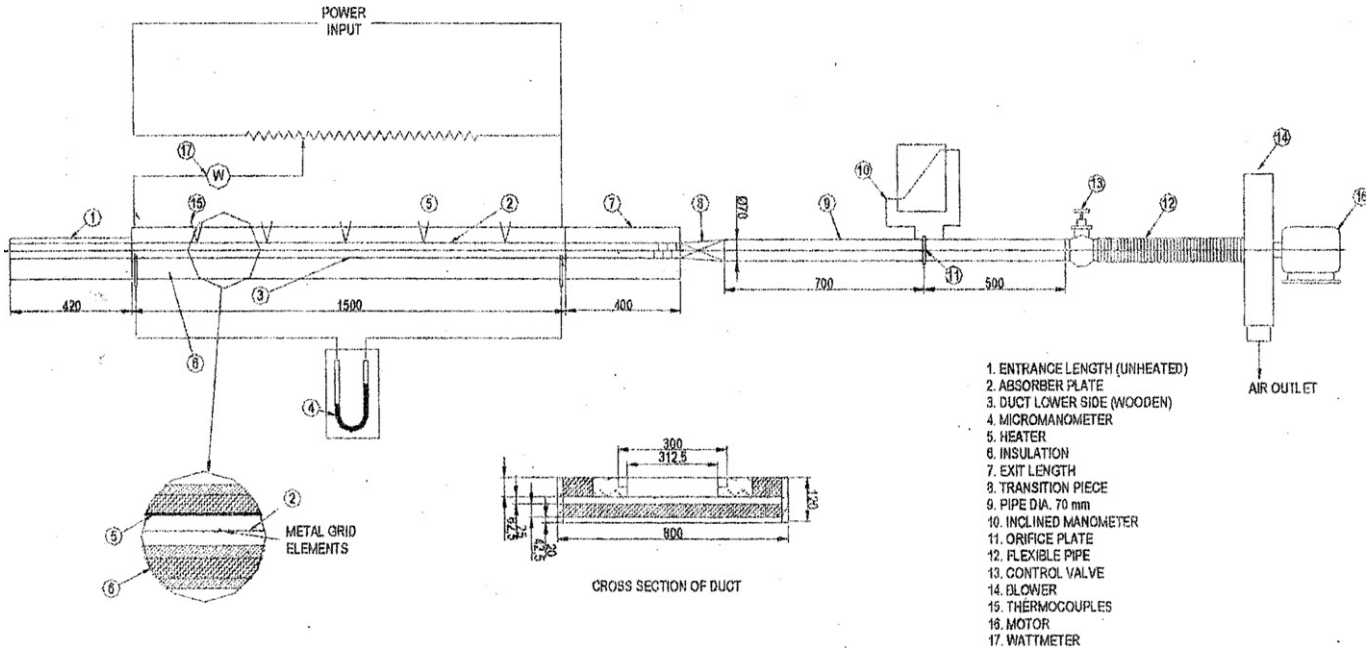

Fig. 1. The schematic layout of experimental setup.

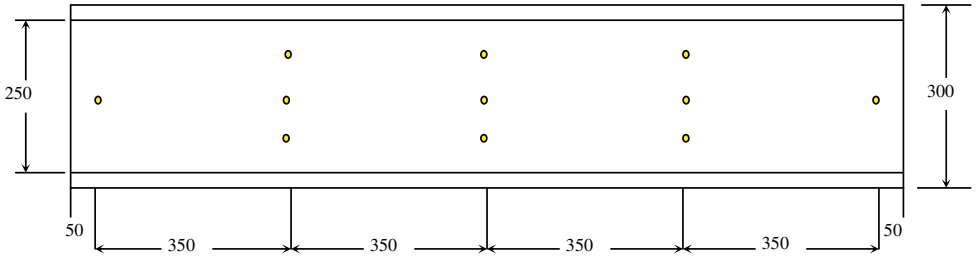

Fig. 2. Thermocouple locations on collector plate.

flow rate of air, is used to determine the values of performance parameters. Mass flow rate (m), heat transfer to the air (q), heat transfer coefficient (h), Stanton number St, and Nusselt number (Nu) in the duct are calculated as:

$$m = C_d A_o \left[\frac{L_f \rho \Delta P_0}{1-\beta^4}\right]^{0.5} \quad (1)$$

$$q = mC_p(T_0 - T_i) \quad (2)$$

$$h = q/A_c(T_{pm} - T_{fm}) \quad (3)$$

A_c is the heat transfer area of the collector plate without ribs. The electric heating gives a constant heat-flux. The plate temperature varies in the direction of the airflow. In all the calculations, a mean plate temperature, T_{pm} is used. The mean plate temperature is calculated as an integral of the mean value of the experimentally measured plate temperatures. T_{fm} is the average fluid temperature.

The Nusselt number and Stanton number are calculated as:

$$St = h/\rho v C_p \quad (4)$$

$$Nu = St\,Re\,Pr \quad (5)$$

The friction factor is determined from the measured value of pressure drop (ΔP_d) across the test section length (L_f),

$$f = \left[\frac{2\Delta P_d D_h}{4\rho L_f V^2}\right] \quad (6)$$

The thermo-physical properties of the air, employed in the calculation of heat transfer and friction factors, are picked up from available standard data tables, which correspond to the average fluid temperature, T_{fm}. The effect of humidity has been neglected since the relative humidity values during experimentation were found to be low and variation was small, ranging between 20% and 32%.

From the analysis of uncertainties in the measurements by various instruments [14], the uncertainties in the calculated values of various parameters are given below.

Reynolds number = ±3.52%.
Friction factor = ±6.12%.
Nusselt number = ±6.36%.
Stanton number = ±7.48%.

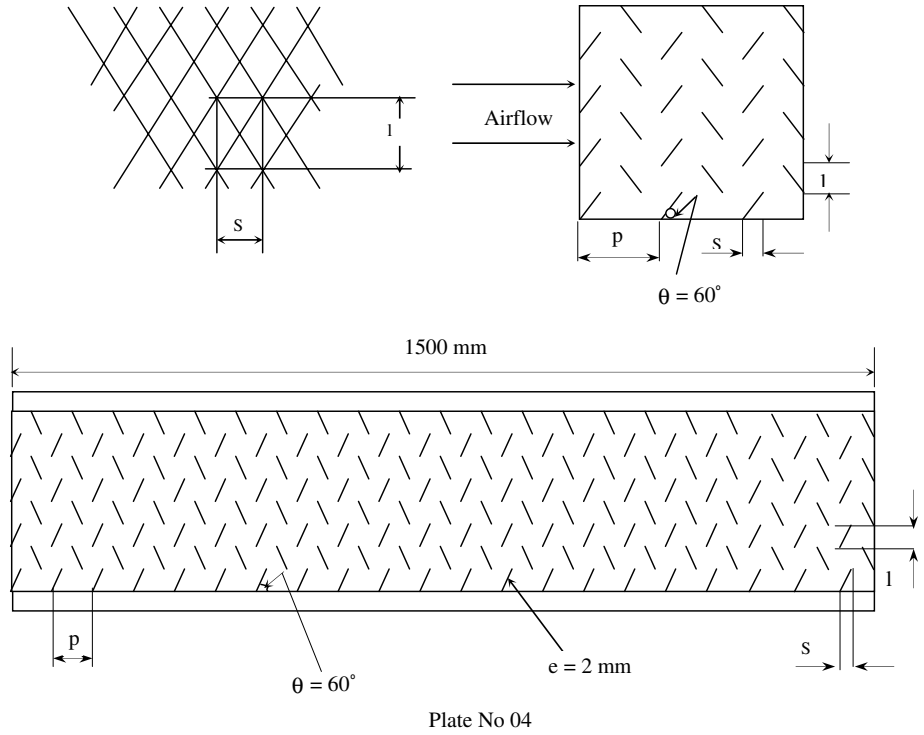

Fig. 3. Geometry of roughened surface collector plate no. 04.

Table 1
Details of the roughened plates

Plate no.	Pitch of metal grids, mm	Diameter of metal grids, mm	Rib angle of attack, °θ	p/e	e/D_h	l/s
02	72	2.0	60	36.0	0.044	1.72
03	48	2.0	60	24.0	0.044	1.72
04	30	2.0	60	15.0	0.044	1.72
05	25	2.0	60	12.5	0.044	1.72
06	35	2.0	60	17.5	0.044	1.72
07	28	1.6	60	17.5	0.035	1.72
08	30	1.7	60	17.5	0.038	1.72
09	26	1.4	50	17.5	0.038	1.23
10	30	1.7	45	17.5	0.038	1.00

2.3. Validity test and experimental results for smooth duct

Experimental values of Nusselt number and friction factor of smooth duct, are compared with the values given in the literature and are shown in Figs. 4a and 4b [15,16]. The Nusselt number correlations of Gnielinski [15] and Dittus and Boelter [16] are given by Eqs. (7) and (8), respectively.

$$Nu = 0.0214(Re^{0.8} - 100)\{1 + (D_h/L)^{0.66}\}(T_{fm}/T_{pm})^{0.45}Pr^{0.4}, \quad \text{for } 2300 < Re < 10^6 \tag{7}$$

$$Nu = 0.024Re^{0.8}Pr^{0.4} \text{ (for heating of fluid)}, \quad \text{for } 10^4 \leqslant Re \leqslant 1.24 \times 10^5 \tag{8}$$

The friction factor for a smooth rectangular duct, given by Bhatti and Shah [16], is as below,

$$f = (1.0875 - 0.1125H/W)fc \tag{9}$$

where, $fc =$ friction factor for the circular duct

$= 0.0054 + 2.3 \times 10^{-8}Re^{1.5}$ for $2300 < Re < 4000$

$= 1.28 \times 0^{-3} + 0.1143Re^{-0.311}$ for $4000 < Re < 10^7$

and the Blasius relation is

$$fc = 0.0791Re^{-0.25} \quad \text{for } 4000 \leqslant Re \leqslant 10^5 \tag{10}$$

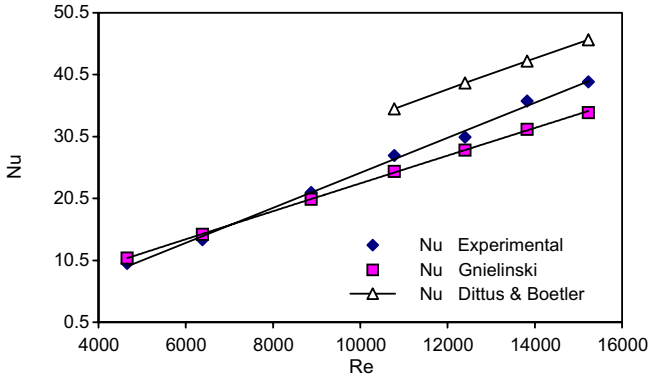

Fig. 4a. Nusselt number by Experimental, Gnielinski, Dittus and Boetler equation vs Reynolds number for smooth duct.

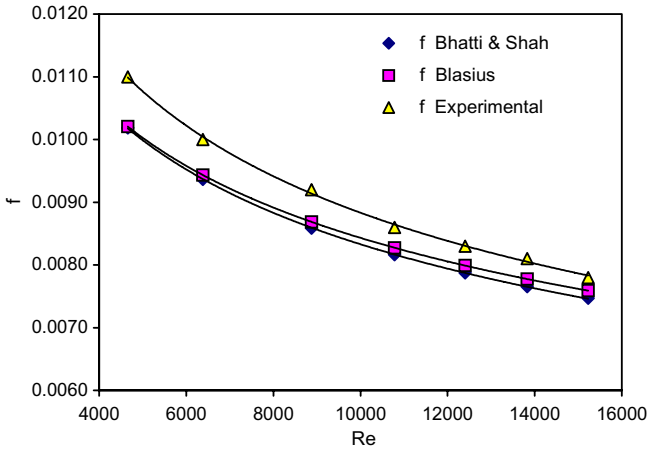

Fig. 4b. Friction factor by experimental, Blkasius and Bhatti and Shah correlation vs Reynolds number for smooth duct.

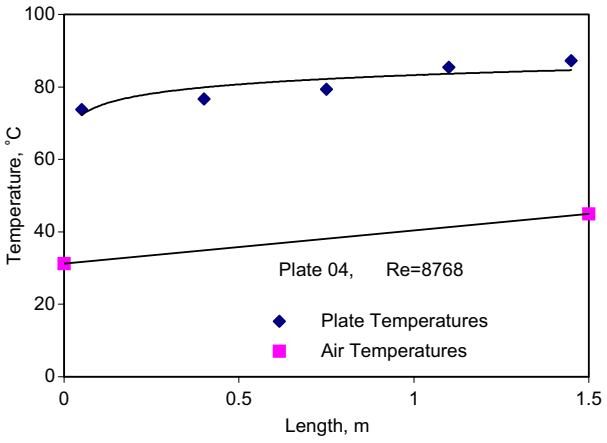

Fig. 5. Plate temperature distributions along the length of the test duct.

The maximum deviation of Nusselt number is found to be 6.5% of the values predicted by Eqs. (7) and (8). The standard deviation of present experimental friction data is found to be ±5.2% for the duct aspect ratio of 10, from the values predicted by Eqs. (9) and (10). Thus, there is a reasonably good agreement between the predicted values, from Eqs. (7) to (10), and the experimental values of the Nusselt number and friction factor. This ensures the accuracy of the experimental data obtained from the present setup.

3. Results and discussion

Fig. 5 shows the variation of temperature of plate and air along the length of roughened test duct. The straight line represents the longitudinal distribution of air temperature. This pattern of temperature variation is similar to that of Han [5] and Karwa et al. [13]. Similar pattern is observed for all collector plates with minor variation of ±0.5 °C. The temperature difference between air and collector plate is observed to be constant from length of 6–8 times hydraulic diameter on downstream side of test section. This indicates that, after 6–8 times hydraulic diameter length, the fully developed temperature profile is established. Thus the entrance region is quite short and the entrance length provided in the present experimental setup is sufficient. It is seen that the $(T_{pm} - T_{fm})$ in the developing region is slightly higher (3 °C) than developed region (30 °C). Thus, heat transfer coefficient in the developing region is 10% higher than that of developed region.

Figs. 6, 7 and 8 show the variation of Nusselt number and friction factor with Reynolds number. Nusselt number and friction factor are the functions of system geometry and operating parameters. The trend shows that Nusselt number increases with Reynolds number, whereas the friction factor decreases and approaches nearly a constant value. It is also observed that the Nusselt number increases with the Reynolds number for the roughened as well as for smooth surfaces, but the rate of increase is more for the roughened surface as compared to the smooth surface. Also, it is observed that the Nusselt number increases with increase in surface roughness. At low Reynolds number, the Nusselt number for all types of surface approach almost same value, which might be due to less disturbance of laminar sub-layer. The laminar sub-layer acts as the major component of resistance for heat transfer. This layer is disturbed by roughened surface at higher Reynolds number; hence the boundary layer thickness reduces. This reduction in the boundary layer thickness increases the heat transfer rate. In addition to this, local contribution to the heat removal by the vortices is originated from the roughness element. The shedding of vortices also causes additional loss of energy resulting in increased friction factor. Thus, the Nusselt number and friction factor for roughened surfaces deviate from that of the smooth surface.

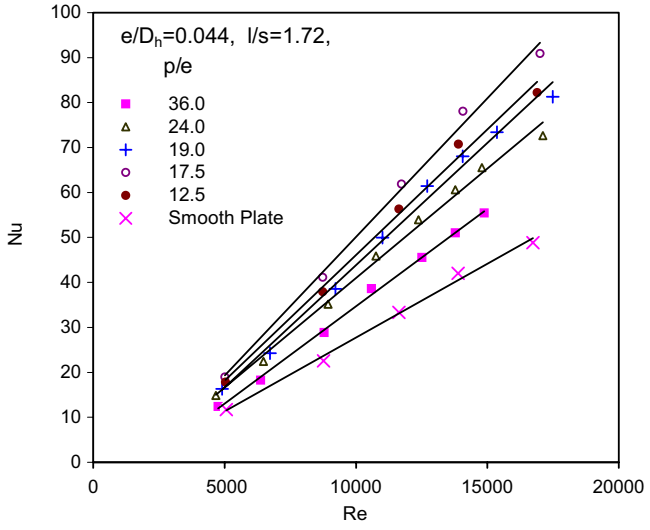

Fig. 6a. Nusselt numbers as a function of Reynolds number for different value of p/e and for fixed value of e/D_h and l/s.

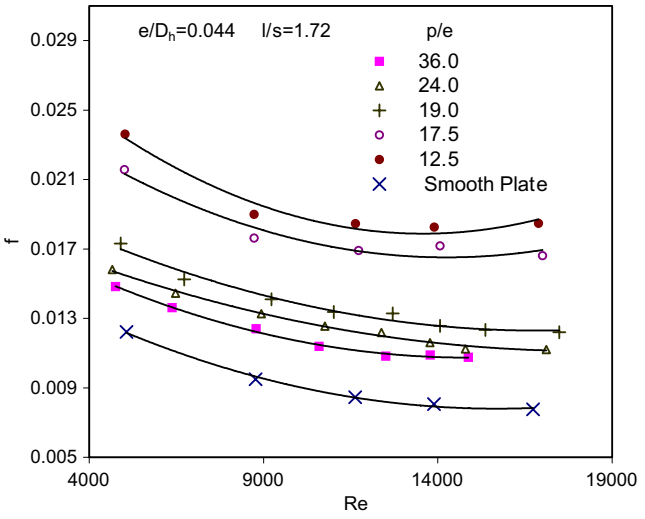

Fig. 6b. Friction factor as a function of Reynolds number for different values of p/e and for fixed value of e/D_h and l/s.

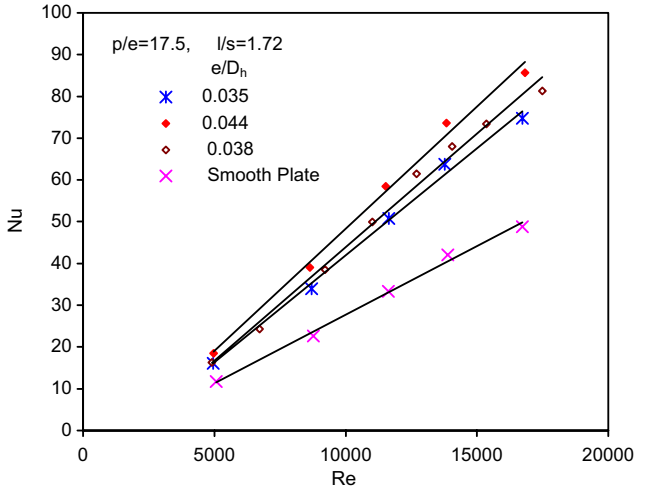

Fig. 7a. Nusselt numbers as a function of Reynolds number for different value of e/D_h and for fixed values of l/s of p/e.

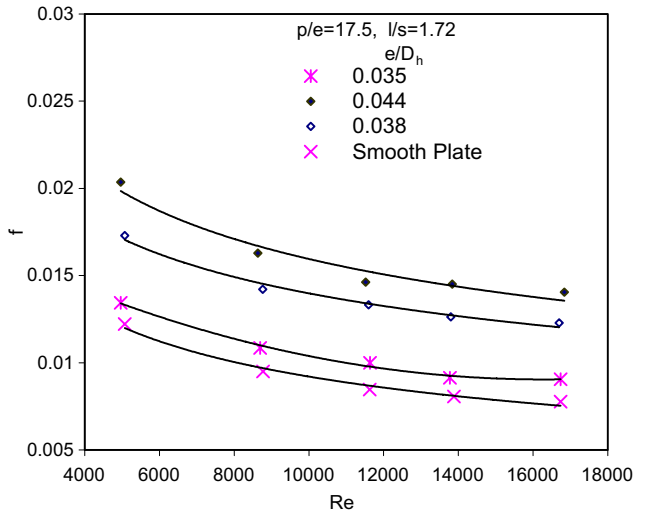

Fig. 7b. Friction factor as a function of Reynolds number for different values of e/D_h and for fixed value of p/e and l/s.

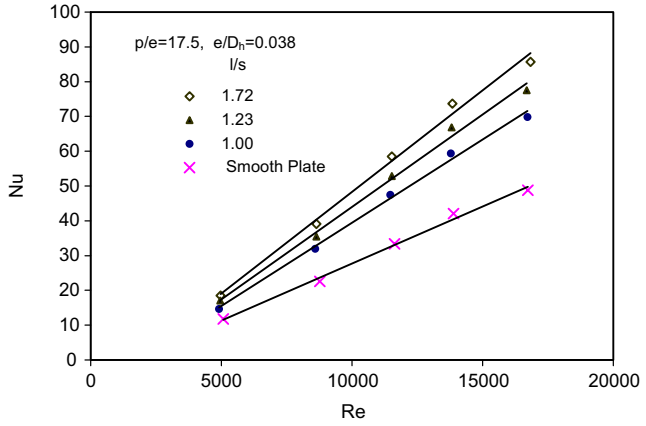

Fig. 8a. Nusselt numbers as a function of Reynolds number for different value of l/s and for fixed values of p/e of e/D_h.

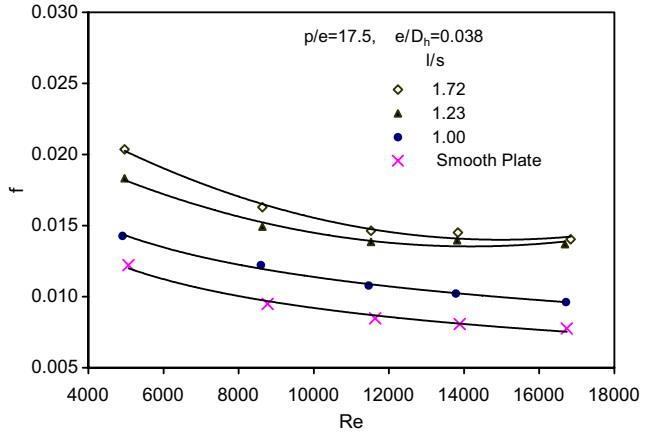

Fig. 8b. Friction factor as a function of Reynolds number for different values of l/s and for fixed value of p/e and e/D_h.

Figs. 6a and 6b depict the Nusselt number and the friction factor as a function of Reynolds number for different values of relative roughness pitch (p/e): 12.5, 17.5, 19, 24, 36 and for fixed value of relative roughness height (e/D_h) 0.044 and relative length of metal grid (l/s) 1.72. Fig. 6a shows that the Nusselt number increases with decrease in relative roughness pitch of metal grid ribs. But at a low relative roughness pitch ($p/e = 12.5$) of metal grit ribs, the rate of increase of Nusselt number decreases. The eddies formed at low value of relative roughness pitch (i.e., $p/e = 12.5$) offer higher degree of disturbance to the laminar sub layer as compared to the roughened surfaces with higher value of p/e and hence the rate of increase of Nusselt number starts decreasing above these roughness values.

The variation of friction factor with Reynolds number is shown in Fig. 6b for different values of relative roughness pitch. The nature of variation is similar for all type of surfaces, but they differ appreciably. It is observed that the surface with roughness parameter $p/e = 12.5$ has maximum roughness factor. However, the surface with roughness

parameter $p/e = 17.5$ has shown maximum heat transfer rate. It mains that, within the boundaries of the experimental work, the surface with roughness parameter $p/e = 17.5$ gives the best performance.

Similarly, Figs. 7a and 7b shows the plots of Nu and f as function of Re for relative roughness height, e/D_h values of 0.035, 0.038, 0.044, and at a fixed value of $l/s = 1.72$ and $p/e = 17.5$. From this plot, it can be observed that the Nusselt number increases with e/D_h, which may be attributed to the increase in roughness height leading to the penetration of roughness elements in the laminar sub-layer, causing increase in Nu.

Figs. 8a and 8b show the similar trend of Nusselt number and friction factor for the roughness parameters (l/s): 1.00, 1.23, 1.72 at a fixed (e/D_h): 0.38 and (p/e): 17.5. These results are in good agreement with those reported by Prasad and Saini [11].

In general, it can be said that the enhancement of heat transfer for any type of rib roughness on the plate surface is caused due to the increased turbulence at adjacent wall. The additional enhancement observed might be due to the contribution of the secondary flow of air along the ribs, which carry the heated air away from the plate surface.

In case of different configurations like inclined, discrete, continuous and V-arrangement of roughened surfaces, the secondary air flows towards the sidewalls of duct. The temperatures are higher on the leading edge side of the ribs than the trailing edge side because of the secondary airflow near the rib side due to the inclinations of the ribs [17]. Such variation in outlet air temperature in transverse direction for continuously inclined, discrete and V-arrangements are found by Karwa et al. [17]. In the present work it is observed that, the temperature variation, in the transverse direction is appreciably low, as shown in Fig. 9. This is caused due to the short distance movement of the secondary airflow. The discrete ribs arrangement causes better mixing of the secondary and primary flows, which results in higher heat transfer rate.

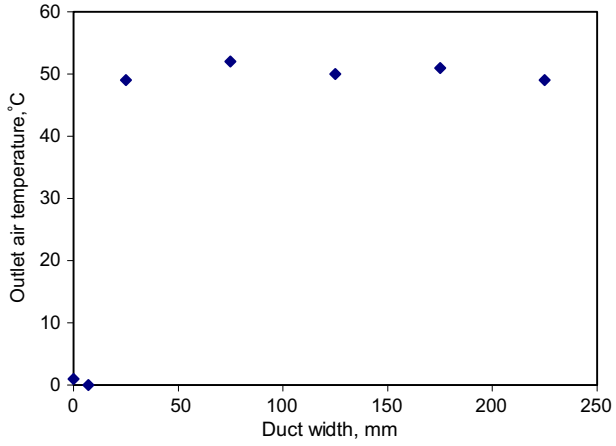

Fig. 9. Variation in outlet air temperature in transverse directions of duct for plate no. 3.

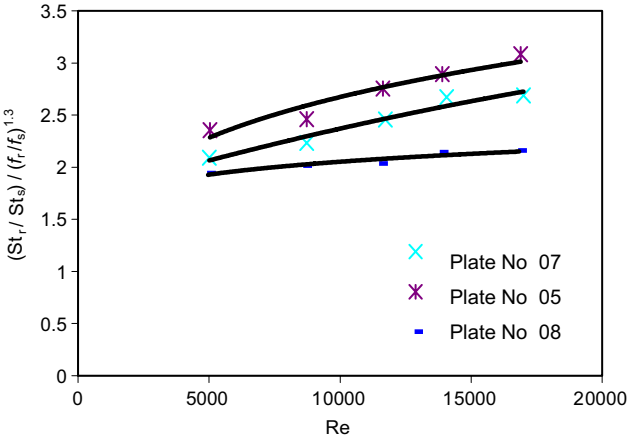

Fig. 10. Thermohydraulic performance vs Reynolds number.

Fig. 10 represents the thermo-hydraulic performance ratio as a function of Reynolds number for the plate numbers 05, 07 and 08, for the search of optimum performance. It is seen that plate number 05 yields higher thermo-hydraulic performance as compared to that of plate number 07 and 08. Hence, parameters of plate number 05 can be used to yield optimum performance for heat transfer and friction characteristics.

4. Correlations for Nusselt number and friction factor

It is seen that Nusselt number and friction factor are effective functions of flow and roughness characteristics, viz., flow Reynolds number (Re) and roughness dimensions of relative length (l/s), relative roughness height (e/D_h) and relative roughness pitch (p/e). The functional relationships for Nusselt number and friction factor can therefore be written as:

$$Nu = f_1(Re, l/s, e/D_h, p/e) \tag{11}$$

$$f = f_2(Re, l/s, e/D_h, p/e) \tag{12}$$

4.1. Correlation for Nusselt number

Fig. 11 depicts the experimental data points represented by Nusselt number vs Reynolds numbers plot. A regression analysis to fit a straight line through data points yields

$$Nu = A_0 Re^{A1} \tag{13}$$

It is seen that the constant A_0 is the function of other influencing parameters. Now taking the relative roughness height of metal grids (e/D_h) as a parameter into consideration, the value of Nu/Re^{A1} ($=A_0$) corresponding to all values of e/D_h is plotted against e/D_h, as shown in Fig. 12. Regression analysis to a straight line through these points yields

$$Nu/Re^{A1} = B_0(e/D_h)^{B1} \tag{14}$$

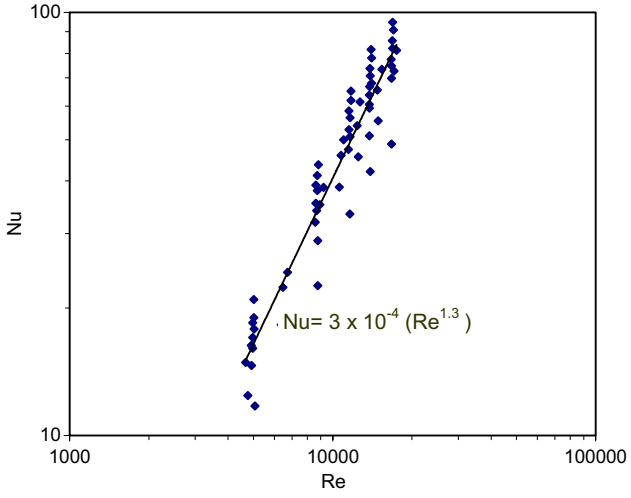

Fig. 11. Plot of Nusselt number vs Reynolds number.

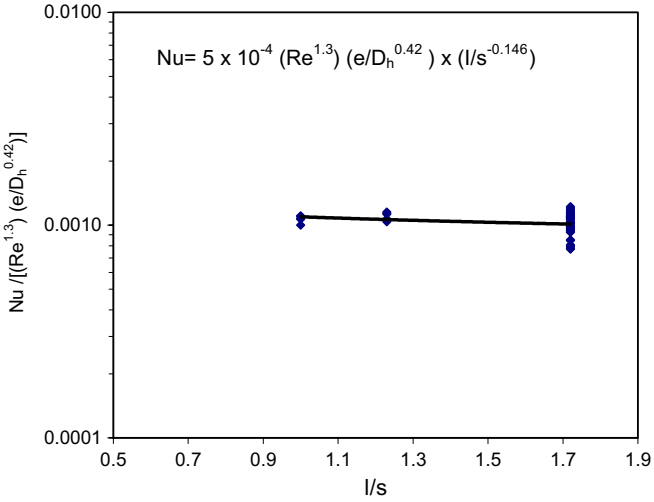

Fig. 13. Plot of $Nu/[(Re^{1.3})(e/D_h^{0.42})]$ vs (l/s).

Such a relationship indicates a group of plots of Nusselt number as a function of relative roughness height of metal grid (e/D_h), each plot being drawn for a given value of flow and all other roughness parameters. Here H_0 is a function of other influencing parameters.

Now, considering the relative length of metal grids (l/s) as a parameter, the value of $Nu/[Re^{A1}(e/D_h)^{B1}](=H_0)$ is plotted against l/s in Fig. 13.

The regression analysis to fit a straight line through these points yields

$$Nu/[Re^{A1}(e/D_h)^{B1}] = C_0(l/s)^{C1} \tag{15}$$

This can be written as

$$Nu/[Re^{A1}(e/D_h)^{B1}(l/s)^{C1}](=C_0)$$

where, C_0 is a function of parameter p/e. Such a relationship indicates the Nusselt number plots, presented as a function of l/s for given values of other parameters.

Finally, a plot of $Nu/[Re^{A1}(e/D_h)^{B1}(l/s)^{C1}](=C_0)$ as a function of parameter p/e, as shown in Fig. 14 used to fit a straight line through data points, yields,

$$Nu/[Re^{A1}(e/D_h)^{B1}(l/s)^{C1}] = D_0(p/e)^{D1}. \tag{16}$$

This can be written as $Nu/[Re^{A1}(e/D_h)^{B1}(l/s)^{C1}(p/e)^{D1}]\times(=D_0)$.

The values of constants $A1$, $B1$, $C1$, $D1$ and D_0 are indicated in Figs. 11–14.

These values result in the following relationship for Nusselt number:

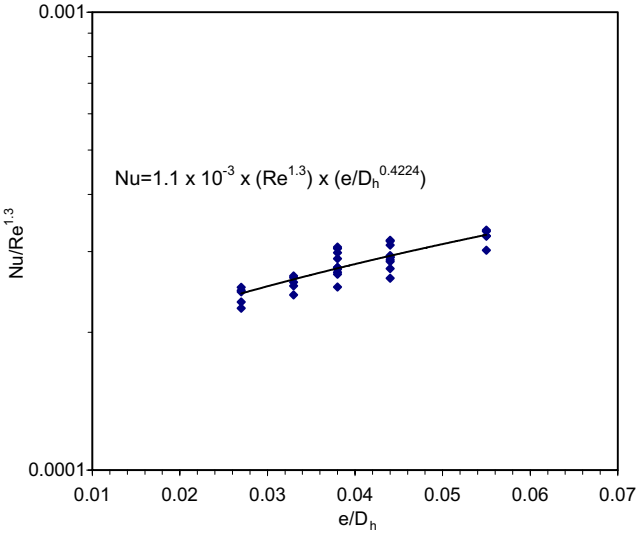

Fig. 12. Plot of $Nu/Re^{1.3}$ vs e/D_h.

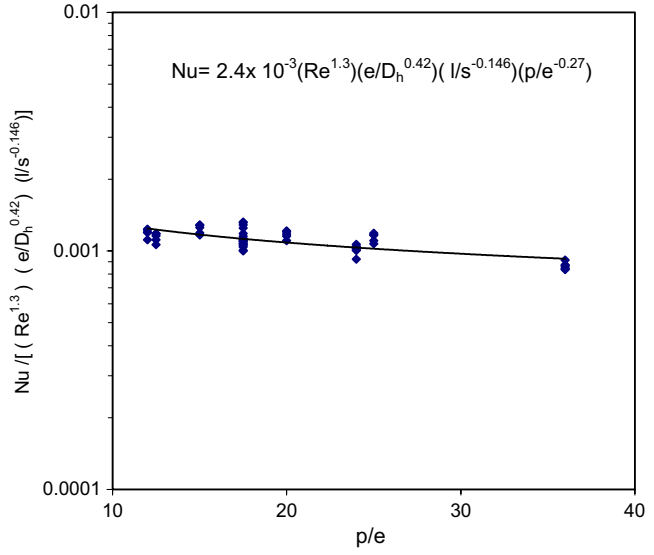

Fig. 14. Plot of $Nu/[(Re^{1.3})(e/D_h^{0.42})(l/s^{-0.146})]$ vs (p/e).

$$Nu = 2.4 \times 10^{-3} \times (Re)^{1.3} \times (e/D_h)^{0.42} \times (l/s)^{-0.146} \times (p/e)^{-0..27} \quad (17)$$

4.2. Correlation for friction factor

A similar procedure is employed and a correlation is developed for friction factor. Figs. 15–18 depict the steps of obtaining such a relationship in the following form:

$$f = 15.55 \times (Re)^{-0.26} \times (e/D_h)^{0.91} \times (l/s)^{-0.27} \times (p/e)^{-0.51} \quad (18)$$

Figs. 19 and 20 show the comparison of Nusselt number and friction factor between the experimental values and those predicted by the respective correlations (17) and (18). The average absolute percentage deviation between the experimental and predicted values is found to be within 2% and 7%.

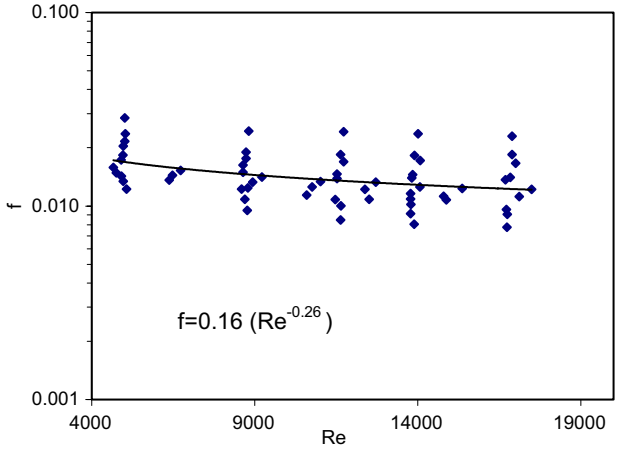

Fig. 15. Plot of friction factor vs Reynolds number.

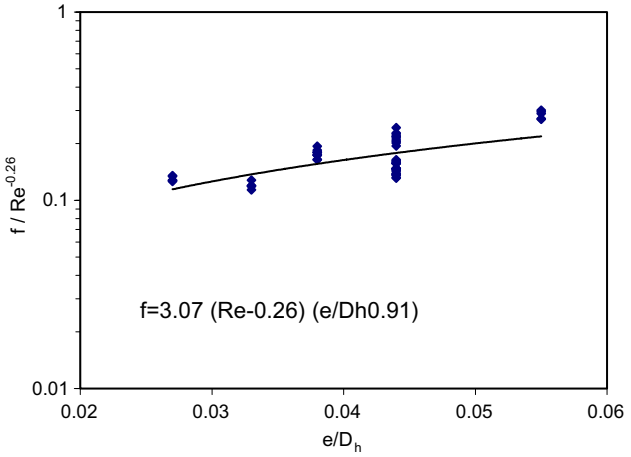

Fig. 16. Plot of $f/(Re^{-0.26})$ vs e/D_h.

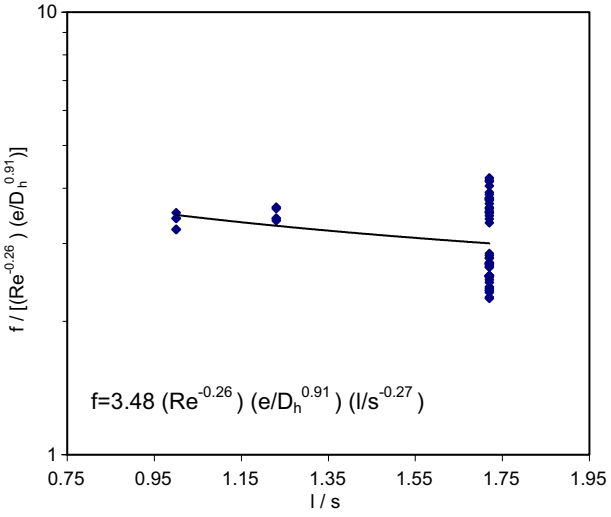

Fig. 17. Plot of $f/[(Re^{-0.26})(e/D_h^{0.91})]$ vs l/s.

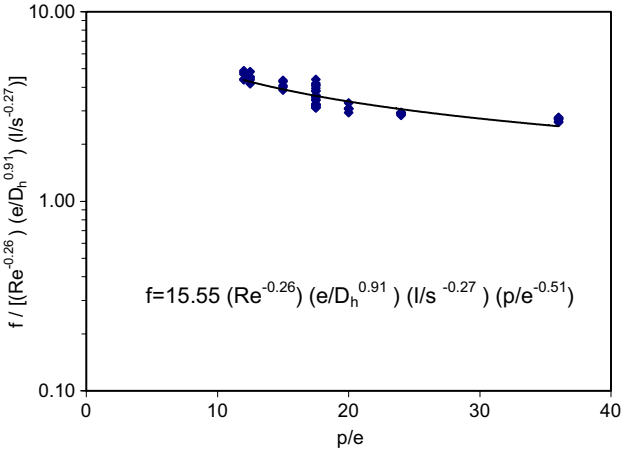

Fig. 18. Plot of $f/[(Re^{-0.26})(e/D_h^{0.91})(I/s^{-0.27)}]$ vs (p/e).

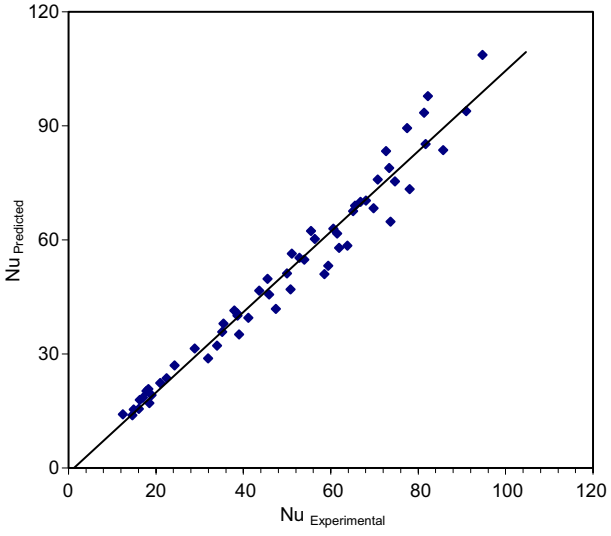

Fig. 19. Plot of predicted values vs experimental values of Nusselt number.

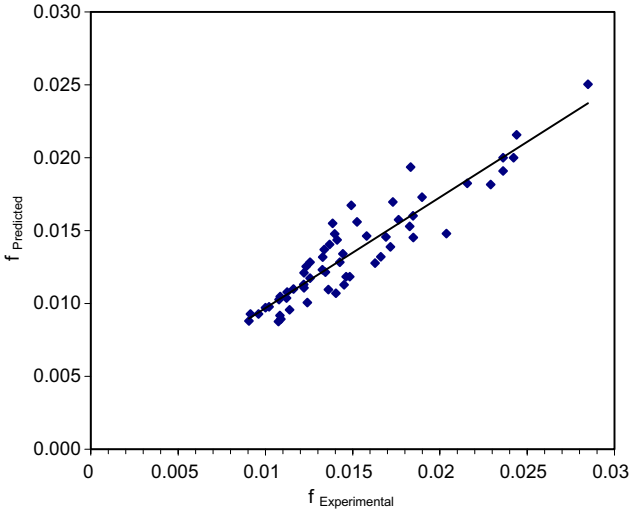

Fig. 20. Plot of predicted values vs experimental values of Nusselt number.

5. Conclusion

This paper presents an experimental investigation of heat transfer performance of a rectangular duct with metal grit ribs as roughness elements employed on one broad wall, transferring heat to the air flowing through it. The broad wall is subjected to uniform heat flux. The effect of relative length, height and pitch of metal grid ribs on the heat transfer and friction factor studied for the flow range of Reynolds numbers 4000–17,000. The main findings of the study are:

1. The presence of metal grit ribs on collector surface of the duct yields up to two-fold enhancement in the Nusselt number and three-fold enhancement in the friction factor, for the range of Re (4000–17,000), l/s (1.00–1.72), e/D_h (0.035–0.044) and p/e (12.5–36).
2. Plate no. 05 [roughness parameters: $l/s = 1.72$, $e/D_h = 0.044$, $p/e = 17.5$] shows the highest heat transfer performance yielding highest heat transfer coefficient, where as Plate No. 06 [roughness parameters: $l/s = 1.72$, $e/D_h = 0.044$, $p/e = 12.5$] yielded highest friction factor.
3. Optimum performance is observed for the Plate no. 05 having roughness parameters $l/s = 1.72$, $e/D_h = 0.044$, $p/e = 17.5$ for the range of parameters studied. (Enhancement in Nusselt number was found to be 187% and the friction factor increased by 213%).
4. Based on the experimental data, correlations are developed for Nusselt number and friction factor. These are fairly in agreement with the experimental and predicted values.

Acknowledgements

Government College of Engineering, Karad and Rajarambapu Institute of Technology, Rajaramnagar, Sakharale supported this research. The authors acknowledge both these institutes for providing facilities.

References

[1] M.H. Hosni, W.C. Hugh, P.T. Robert, Measurement and calculations of rough wall heat transfer in the turbulent boundary layer, Int. J. Heat Mass Transfer 34 (1991) 1067–1082.
[2] J. Nikuradse, Laws of flow in rough pipes, NACA, Technical Memorandum 1292, November 1950.
[3] W. Nunner, Heat transfer and pressure drop in rough tubes, VDI ForschHft, 455-B, 5-39, A.E.-R.E. Lib. Trans. 786, 1958.
[4] D.F. Dipprey, R.H. Sabersky, Heat and momentum in smooth and rough tubes at various Prandtl numbers, Int. J. Heat Mass Transfer 6 (1963) 329–353.
[5] J.C. Han, Heat transfer and friction in a channel with two opposite rib roughened walls, Int. J. Heat Transfer 106 (1984) 774–781.
[6] R.L. Webb, E.R.G. Eckert, Application of rough surfaces of heat exchanger design, Int. J. Heat Mass Transfer 5 (1972) 1647–1658.
[7] J.C. Han, Y.M. Zhang, High performance heat transfer ducts with parallel broken V shaped broken ribs, Int. J. Heat Mass Transfer 35 (1992) 513–523.
[8] T. Liou, J. Hwang, Effect of ridge shapes on turbulent heat transfer and friction in a rectangular channel, Int. J. Heat Mass Transfer 36 (1993) 93–140.
[9] K. Prasad, S. Mullick, Heat transfer characteristics of a solar air heater used for drying purposes, Appl. Energ. 13 (1983) 83–98.
[10] B.N. Prasad, J.S. Saini, Effect of artificial roughness on heat transfer and friction factor in solar air heater, Solar Energ. 41 (1988) 555–560.
[11] R.P. Saini, J.S. Saini, Heat transfer and friction factor correlations for artificially roughened duct with expanded metal mesh as roughness element, Int. J. Heat Mass Transfer 40 (1997) 973–986.
[12] ASHRAE standard 93-77, Method of testing of determine thermal performance of solar collector, 1977.
[13] R. Karwa, S.C. Solanki, J.S. Saini, Heat transfer coefficient and friction factor correlation for the transitional flow regime in rib roughened rectangular ducts, Int. J. Heat Mass Transfer 42 (1999) 1597–1615.
[14] S.J. Kline, F.A. McClintock, Describing uncertainties in single sample experiments, Mech. Eng. 75 (1953) 3–8.
[15] V. Gnielinski, New equation for heat and mass transfer in turbulent heat channel flow, Int. J. Chem. Eng. 16 (2) (1976) 359–367.
[16] M.S. Bhatti, R.K. Shah, Turbulent and transitional flow convective heat transfer, Hand Book of Single-phase Convection Heat Transfer, John Wiley and Sons, New York, 1987 (Chapter 4).
[17] R. Karwa, S.C. Solanki, J.S Saini, Heat transfer and fluid flow characteristics of rectangular ducts with inclined chamfered rib roughness on one broad wall, in: 14th National Heat and Mass Transfer Conference and 3rd ISHMT-ASME. Heat and Mass Transfer Conference at IIT Kanpur, 1997, pp. 331–336.